

Surface Chemical Groups of Flocs Are Key Factors for the Growth of Flocs in Sweep Coagulation: A Case Study of Surface Occupation by Humic Acid

Mengjie Liu and Wenzheng Yu*



Cite This: <https://doi.org/10.1021/acsestengg.2c00229>



Read Online

ACCESS |

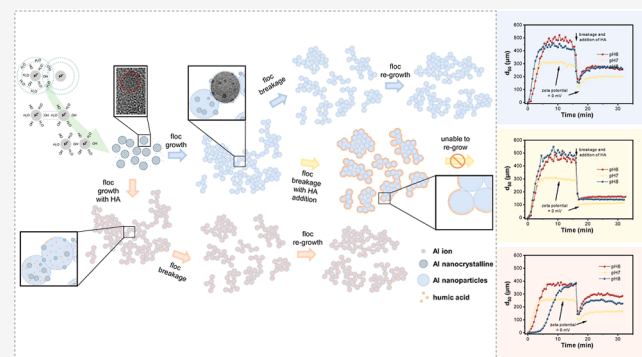
Metrics & More

Article Recommendations

Supporting Information

ABSTRACT: Coagulation is one of the most common processes in water treatment. Charge neutralization and sweep flocculation are recognized as the primary coagulation mechanisms. However, in-depth understanding on floc growth, breakage, and regrowth is still unclear. In this study, the formation, breakage, and regrowth of alum flocs with humic acid (HA) added either before coagulant addition or during the floc breakage stage were investigated. The floc size continuously decreased with the increase in floc breakage events, and eventually, to a stable value. The floc growth was not affected by the addition of HA before coagulant addition. However, it was prevented as HA was added during the breakage stage, and the prevention extent increased with HA dose. Similar results were also found for natural organic matter (NOM) from real surface water. These results suggested that HA/NOM can cover the active site on the floc surface, and the coverage differed for fresh flocs (newly precipitated) and old flocs (after breakage), which, respectively, represent the case in conventional coagulation and sludge recirculation. Based on these findings, the illustration of floc growth, breakage, and regrowth processes was put forward. We concluded that the charge neutralization and sweep flocculation mechanisms only explained the possibility of flocs approaching each other; whether flocs can connect to each other depends on the activated functional groups on the floc surface. The results in this study revealed the underlying mechanism of “collision effectiveness” in coagulation, complementing the existing understanding of the coagulation process.

KEYWORDS: alum floc, floc breakage, floc regrowth, humic acid, adsorption



1. INTRODUCTION

Coagulation, with the benefits of low cost and broad application, is one of the most common processes in water treatment.^{1–5} Among various coagulant products,^{6–9} hydrolyzing metal salts such as alum and ferric salts are most widely used. It has long been recognized that charge neutralization and sweep flocculation are two important mechanisms for coagulation.^{10,11} However, the in-depth understanding of the floc growth process was still unclear.

It is now well established that hydroxide flocs formed with hydrolyzing coagulants may show irreversible breakage, that is, the flocs broken at higher shear rates do not fully regrow to previous size after the shear rate reduced to previous value.¹² This behavior is found for the coagulation of both particulate suspensions (e.g., clays) and natural organic matter (NOM) [e.g., humic acid (HA) and natural waters].^{13,14} Even after several floc breakage and regrowth cycles, the size of the regrown flocs continues to decrease, before eventually reaching a limiting value.¹⁵ A number of previous studies have drawn some insightful conclusion on floc interactions and the growth process.^{16–18} For instance, it was found that different

coagulants produce flocs with different morphologies,¹⁹ thus affecting the degree of recovery from shearing.¹⁴ The effect of physical properties such as floc size, compaction, and strength on floc breakage and regrowth has also been explored.^{13,19,20}

Chemical properties, such as surface functional groups and crystallization of flocs, were also found responsible for the regrowth ability.²¹ A study showed that the $\text{Al}(\text{OH})_3$ precipitate loses 75% of its adsorption capacity for phosphate after aging.²² Therefore, repeated small doses of alum may be more effective than a single large dose in coagulation. Our previous work also observed that when adding a small additional dosage of the coagulant during floc breakage, the regrown flocs can be at least as large as those before

Received: July 6, 2022

Revised: September 20, 2022

Accepted: September 21, 2022

breakage,^{23,24} which implied that the addition of the coagulant was able to promote the regrowth of broken flocs. However, this effect is only found when the additional coagulant contains mainly monomeric Al species (Al_a). If a prehydrolyzed coagulant such as polyaluminum chloride (PACl) is used, containing mainly polymeric forms, such as “ Al_{13} ” (Al_b), then there is no improvement in floc regrowth.²⁴ Therefore, the differences in surface chemical groups of the primary particles should be responsible for the floc regrowth ability.²⁵

Despite a great number of studies discussing the properties of flocs and their effects on floc growth behavior and some of them using NOM as raw solution, little attention has been paid to the role of NOM in floc growth behavior. NOM, as a predominant target contaminant and participant in coagulation, plays an essential role in coagulation efficiency.^{26–28} Several studies indicated that the direct chemical reaction and adsorption of NOM onto metal precipitates could reduce its growth¹³ and lead to a significant reduction in the regrowth ability of broken flocs.²⁹ These results suggested that the surface of broken flocs may be changed by HA. However, the mechanism has not been explored yet. Therefore, the present work focuses on the floc breakage and regrowth process, exploring the effect of HA adsorption on floc surface properties and how it affects the regrowth of broken flocs. The results of this study revealed the floc growth process at the existence of NOM and complement the existing coagulation mechanism.

2. MATERIALS AND METHODS

2.1. Stock HA and Coagulant Solutions. Suwannee River HA (2S101H, International Humic Acid Substance Society, USA) was dissolved in deionized (DI) water and was mixed by a magnetic stirrer for 24 h to prepare a 5 g/L HA stock solution, with pH adjusted to 7.5 by 0.1 M HCl. The solution was stored in the dark before use. The aluminum sulfate hydrate ($\text{Al}_2(\text{SO}_4)_3 \cdot 18\text{H}_2\text{O}$) analytical reagent is one of the most widely used coagulants in the drinking water treatment plant^{30,31} and is used in this study. The stock alum solution at a concentration of 0.1 M (0.2 M Al) was prepared using DI water.

2.2. Jar Test. A beaker (capacity 1.2 L) with a flocculator (ZR4-2, Zhongrun, China) was used for jar test, which enabled the mixing speed and duration to be preset. After adding a certain dosage of alum (0.2 mM), the stirring speed was set to 200 rpm (mean velocity gradient, G of 184 s^{-1}), and maintained for 1 min (rapid mixing stage). Subsequently, the stirring speed was reduced to 50 rpm (G of 23 s^{-1}) to allow floc growth (floc growth stage). After 15 min of slow stirring, the speed was increased to 200 rpm for 1 min to facilitate floc breakage (floc breakage stage), and then, the speed rate was decreased back to 50 rpm for 15 min for the regrowth of broken flocs (floc regrowth stage). This cycle of floc formation, breakage, and regrowth was repeated several times.

During the jar test, the pH of the solution was maintained at the desired value by prior addition of 0.1 M HCl and 5 mM NaHCO_3 . The different addition modes of alum and HA for the experiments were as follows: alum was first added without HA to form the alum precipitate and 5 mg/L HA was added at the middle of the first or third floc breakage stage. For comparison, a solution of 5 mg/L HA was also added before the addition of the coagulant to coagulate with alum. The temperature was maintained at $25 \pm 2^\circ\text{C}$ during all experiments.

2.3. Jar Test Using Natural Surface Water. The local nature surface water, collected from the JingMi river (JM), Beijing, China, was used in this study. JM river is a channel providing drinking water for Beijing.³² The physical and chemical properties of JM water are shown in Table S1 (Supporting Information). The JM water was filtered through the 0.45 μm membrane and stored at 4°C before use. A nanofiltration membrane (NF90, RisingSun Membrane Technology (Beijing) Co., Ltd., China) was used to concentrate the JM water. The properties of the NF90 membrane are shown in Table S2 (Supporting Information). Briefly, 2.5 L of JM water was filtered through the membrane in a dead-end filtration apparatus (Amicon 8400, Millipore, USA), and the last 50 mL of concentrated water above the membrane was used in the following jar test.

The jar test procedure was the same as mentioned above, except for the fact that concentrated JM water with different doses was added rather than the HA stock solution. Moreover, the JM water was used to coagulate with alum as a comparison.

2.4. Floc Monitoring. A laser diffraction instrument (Malvern Mastersizer 2000, Malvern, U.K.) was used to measure the dynamic floc size as the coagulation process proceeded. The size range measured by the instrument is between 0.02 and 2000 μm . The suspension was drawn through the optical unit of the Mastersizer and then went back into the jar via a peristaltic pump. The inflow and outflow tubes were positioned at the depth just above the paddle. Size measurements were taken every half minute, and the floc sizes were recorded as volume median values- d_{50} . This type of arrangement has previously been successfully applied to the analysis of flocs by Jarvis et al.,¹³ as well as in our previous work.³³ Flocs were pumped at a flow rate of 2.0 L/h. Preliminary experimentation showed that flow rates above this value gave rise to floc breakage, while below this rate, flocs settled in the tubing. The floc fractal dimension can be calculated from the scattered light intensity (I) and scattering vector (Q). Detailed information was mentioned in our previous study.³³ In brief, the total scattered light intensity I is a function of the scattering vector Q and fractal dimension D_f (eq 1)

$$I \propto Q^{D_f} \quad (1)$$

where Q is the difference between the incident and scattered wave vectors of the radiation beam in the medium, which is given by eq 2

$$Q = \frac{4\pi n \sin\left(\frac{\delta}{2}\right)}{\lambda} \quad (2)$$

where n is the refractive index of the suspending medium, δ is the scattering angle, and λ is the wavelength of the radiation in a vacuum.

2.5. Other Analytical Methods. UV absorbance at 254 nm (UV_{254}) was determined using an ultraviolet/visible spectrometer (U-3010 Hitachi High-Technologies Co., Japan) after 0.45 μm membrane filtration. A 3D excitation-emission matrix (EEM) spectrofluorometer (F-4600FL, Hitachi, Japan) was used to characterize fluorescent organic substances in water samples. The molecular weight (MW) distribution was determined by size exclusion chromatography (SEC) equipped with an optical detector (Waters, USA). Total organic carbon (TOC) was measured using a TOC analyzer (TOC-Vwp, Shimadzu, Japan). Residual dissolved Al concen-

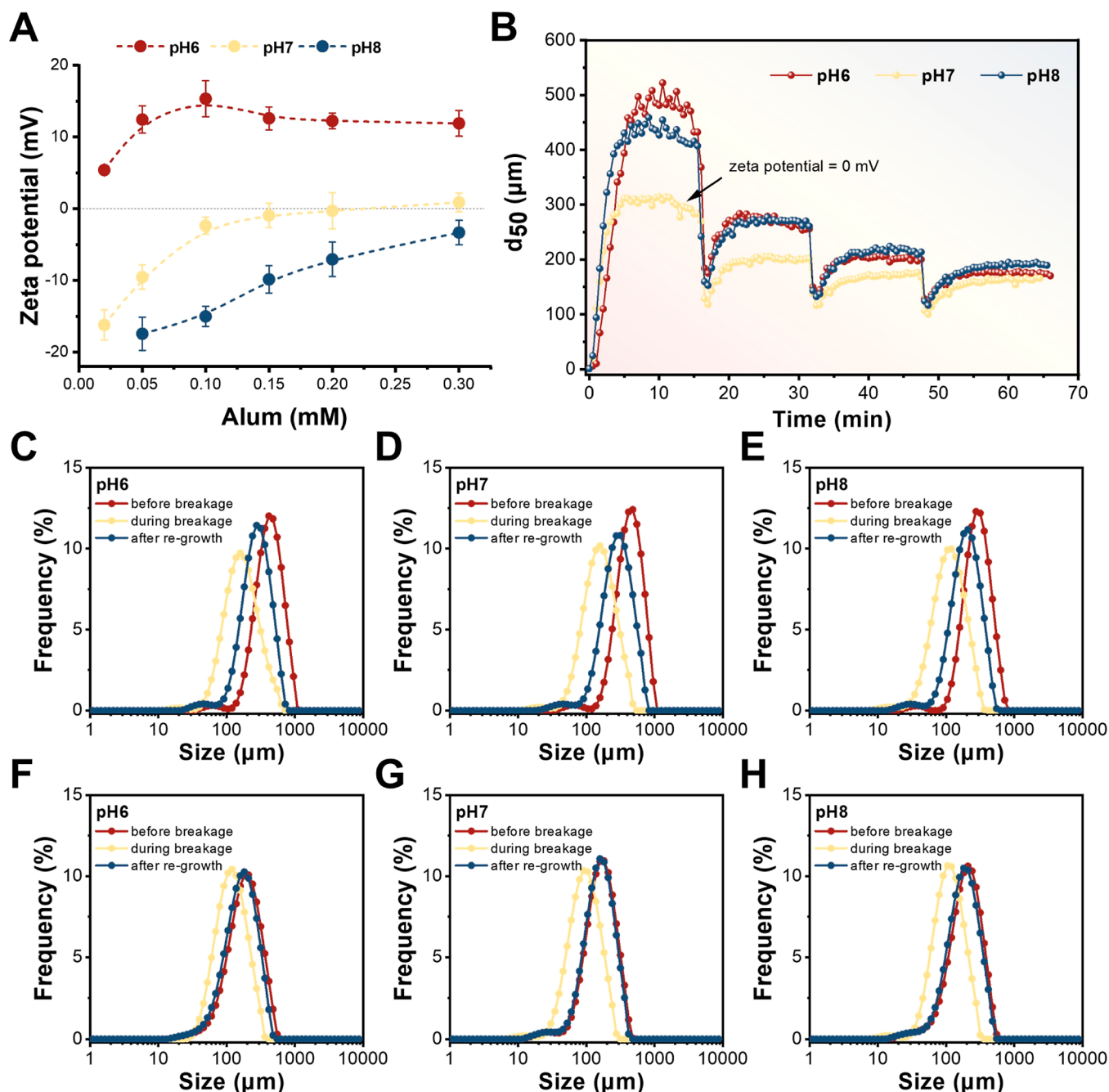


Figure 1. Floc growth, breakage, and regrowth without HA. (A) Effect of pH and alum concentration on the zeta potential of flocs; (B) variation of d_{50} with coagulation time at pH 6 (red), pH 7 (yellow), and pH 8 (blue); (C–E) size distribution of flocs during the first breakage stage at pH 6 (C), pH 7 (D), and pH 8 (E); and (F–H) size distribution of flocs during the third breakage stage at pH 6 (F), pH 7 (G), and pH 8 (H). In (B–H), flocs were formed at 50 rpm for 15 min and then broken at 200 rpm for 1 min. Alum dosage was 0.2 mM.

trations (after 0.45 μm membrane filtration) were determined by inductively coupled plasma-atomic emission spectroscopy (ICP-OES; Optima 2000DV, Perkin-Elmer, USA). Samples after 1 min rapid mixing in the jar test were immediately taken for zeta potential measurements (Zetasizer nano ZS90, Malvern, UK). The flocs were dried in air and then observed by transmission electron microscopy (TEM) (H-7500, Hitachi).

3. RESULTS AND DISCUSSION

3.1. Floc Growth, Breakage, and Regrowth without HA.

When alum was added in water, it hydrolyzed immediately

and formed flocs. As shown in Figure 1B, the size of flocs increased rapidly and reached a plateau after 5 min of stirring, reaching a balance between aggregation rate and breakage rate.^{13,34} It is well-known that both coagulant dose and pH are important factors that affect the coagulation performance. The zeta potential of alum precipitates at different alum doses under different pH values is shown in Figure 1A. The zeta potential became more negative as pH increased from 6 to 8 for all alum doses, which is the characteristic of oxide surfaces. As the dosage of alum increased, the zeta potential of flocs changed quickly at first and then became relatively constant, especially at pH 6. The alum dosage was chosen as 0.2 mM for

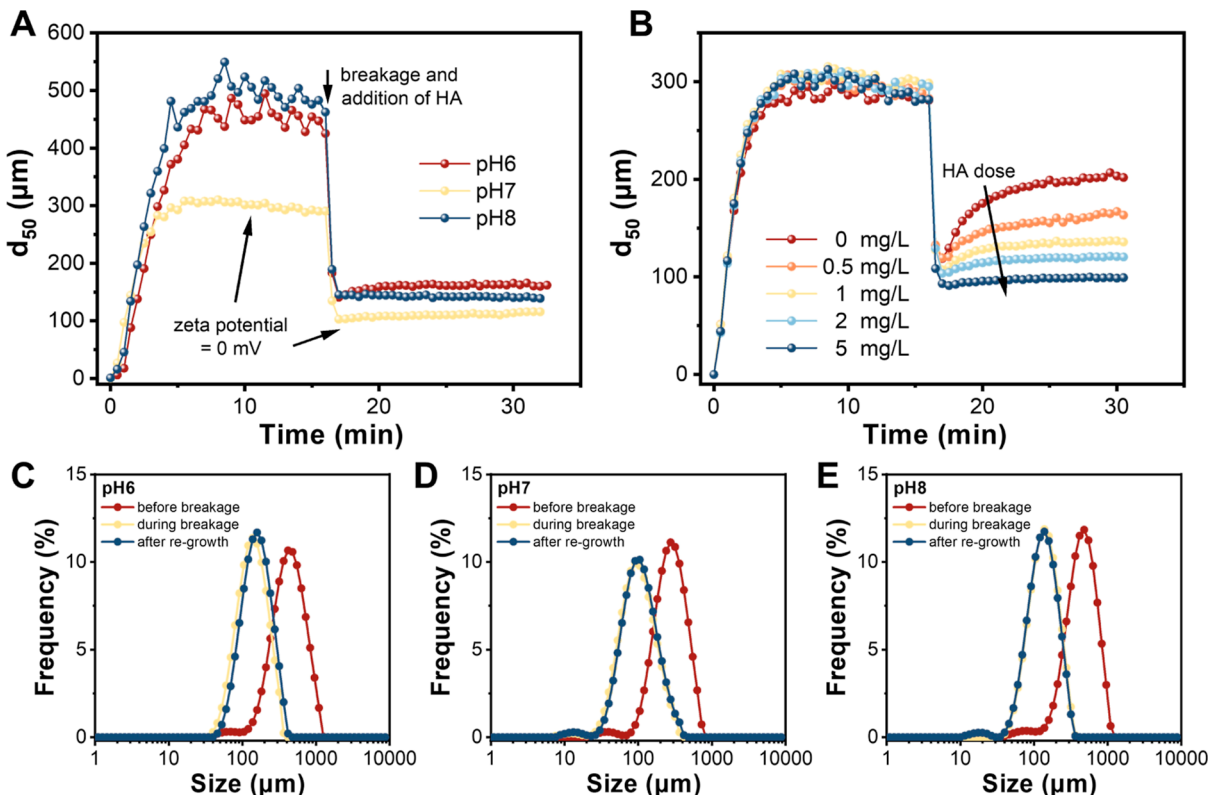


Figure 2. Floc growth, breakage, and regrowth with HA added at the first breakage stage. (A) Variation of d_{50} with coagulation time at pH 6 (red), pH 7 (yellow), and pH 8 (blue) with 5 mg/L HA added at the first breakage stage; (B) variation of d_{50} with coagulation time at pH 7 with 0–5 mg/L HA added at the first breakage stage; and (C–E) size distribution of flocs during the first breakage period at pH 6 (C), pH 7 (D), and pH 8 (E) with 5 mg/L HA added at the first breakage stage. Flocs were formed at 50 rpm for 15 min and then broken at 200 rpm for 1 min. Alum dosage was 0.2 mM.

all of the experiments as the zeta potential of flocs was in the approximate range ± 10 mV at pH 6–8. Moreover, the zeta potential was near zero at pH 7, where the electrostatic repulsion between flocs was the lowest. As a consequence, the initial rate of floc growth was the highest at pH 7 (Figure 1B). However, the average size of stabilized flocs at pH 7 was the lowest among three pH conditions, indicating that zeta potential does not determine the final floc size.

When the stirring speed suddenly increased to 200 rpm, the balance between floc growth and breakage changed, so that the flocs were broken and their size decreased dramatically. Figure 1C–E demonstrates size distribution of flocs during the first breakage stage. After a significant decrease in floc size during the floc breakage stage, the floc size gradually increased at a stirring speed of 50 rpm (floc regrowth stage). However, the average floc size (d_{50}) after regrowth was unable to return to the value before breakage, which suggested that the breakage of flocs was irreversible, and the connection between flocs involves chemical bonds rather than just a physical process.^{13,35} Our previous study suggested that after the breakage of hydroxide flocs, the certain areas of the surface of the floc fragments became “inactive”, so that they do not easily form attachments with other broken flocs.³⁵ As the breakage-regrowth process is repeating, the d_{50} declined continuously, which was similar to the phenomenon observed previously with alum-kaolin flocs.¹⁵ At the third breakage stage, the size of broken flocs almost came back to the value before breakage, implying that the active sites on flocs to form chemical

connections were almost consumed after several breakages (Figure 1F–H).

3.2. Floc Growth, Breakage, and Regrowth with HA.

In water treatment, humic substances are often removed by coagulation with alum or other coagulants. At around neutral pH, the coagulation mechanism was primarily sweep flocculation, that is, the humic substances were removed from water through the absorption on precipitated hydroxide.¹¹ When HA was added with alum before coagulant addition (Figure S1, Supporting Information), the floc growth results were similar to those without HA in Figure 1B, except for smaller plateau d_{50} values compared to alum flocs alone under all pH conditions. Besides, the onset of significant floc growth is delayed by several minutes at pH 8. After the floc breakage stage, the situation was similar to that for alum alone: the flocs gradually regrew, but the plateau d_{50} value could not increase to the value before breakage. Nonetheless, when 5 mg/L HA was added at the floc breakage stage before regrowth (Figure 2A), it was striking that very little or no floc regrowth occurred after the breakage, irrespective of the pH value (Figure 2C–E). Similar situation also occurred when HA was added at the third breakage (Figure S2, Supporting Information): the broken flocs can partly regrow after the first two breakages without the addition of HA, but the regrowth was inhibited by the addition of HA at the third breakage stage. All these results suggested that HA could inactivate the broken flocs and prevent them from regrowth. Moreover, the dose of HA at the breakage stage could affect the extent of inhibition on floc regrowth. For HA dose above 2

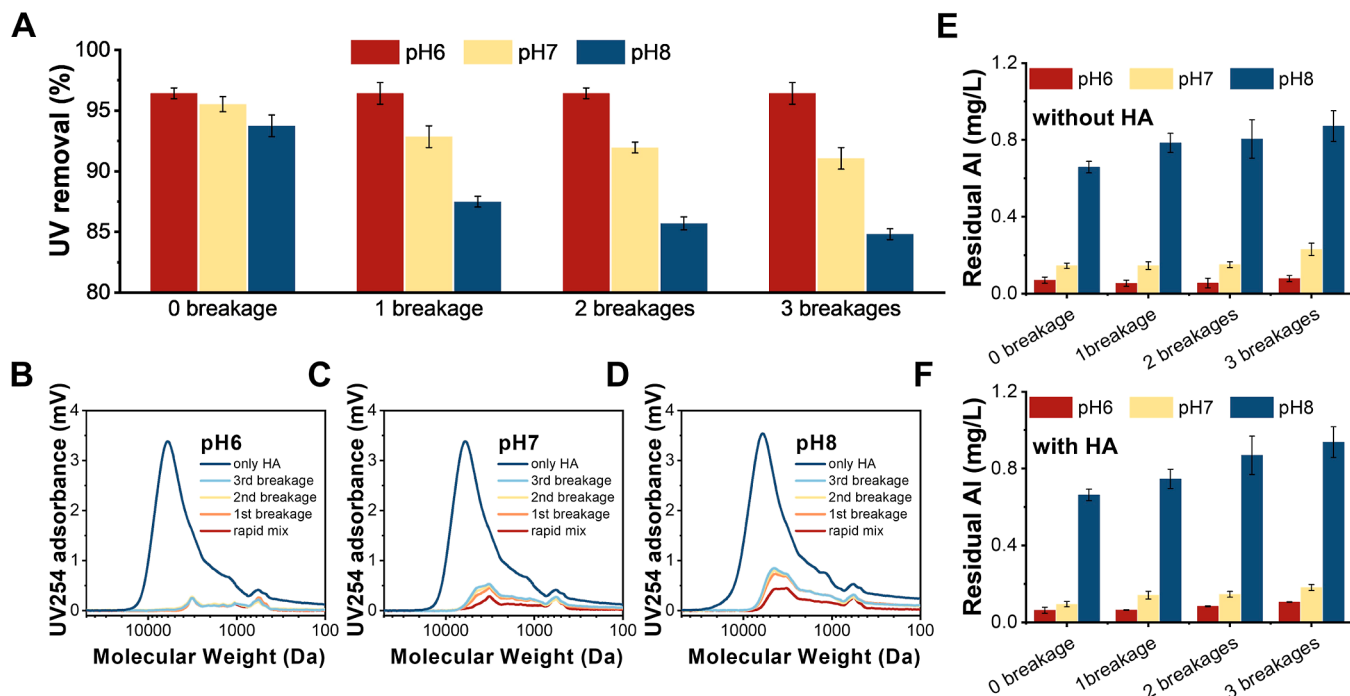


Figure 3. Effect of floc breakages and pH on the adsorption of HA and residual Al. (A) UV₂₅₄ removal rate under different pH values with 5 mg/L HA added at different breakage stages, noting that 0 breakage meant that HA was added before coagulant addition; (B–D) molecular weight distribution under different pH values with 5 mg/L HA added at different coagulation stages: pH 6 (B); pH 7 (C); and pH 8 (D); and (E,F) residual Al without (E) and with (F) the addition of HA (5 mg/L) at different times of breakage. Flocs were formed at 50 rpm for 15 min and then broken at 200 rpm for 1 min. Alum dosage was 0.2 mM.

mg/L, there was little regrowth of broken flocs, while for HA with low dose (<2 mg/L), the regrowth ability of broken flocs increased with the decrease in HA dose (Figure 2B). Figure S3 (Supporting Information) also shows that as HA dose increased, the size distribution of regrown flocs was getting close to the size of broken flocs, until there was no change in size by adding 5 mg/L HA.

3.3. NOM Removal and Residual Al before and after Breakage. In order to examine the effect of floc breakage on NOM removal, the UV₂₅₄ removal rate and the molecular weight (MW) distribution of HA were measured after different floc breakage cycles (Figure 3A–D). HA was added either before coagulant addition (referred as 0 breakage in Figure 3A) or during the first, second, or third breakage stage (corresponding to 1 breakage, 2 breakages, and 3 breakages, respectively, in Figure 3A). When pH was 6, the adsorption capacity of the Al precipitate for HA is not affected by floc breakage. However, when pH was 7 or 8, the UV₂₅₄ removal decreased with increasing number of breakages, especially after the first breakage, which corresponded with the greatest decrease in floc size (Figure 1B). The decrease in NOM removal was especially noticeable for the results at pH 8. Similar results were also obtained from the MW distribution in Figure 3B–D. Coagulation showed great removal of molecules with high MW (>1000 Da). Little increase in NOM was noticed after several breakages at pH 6, but a significant increase in NOM (MW in the range of 1000–10000 Da) with breakage times was found for pH 7 and 8. It was known that pH can affect the charge on NOM and flocs. When pH increased from 6 to 8, the zeta potential gradually decreased from a positive value to negative value. Meanwhile, the carboxyl and hydroxyl groups on NOM carried negative charges. Consequently, the electrostatic repulsion between

flocs and NOM resulted in a low removal rate under high pH. Besides, the effect of pH on HA (or UV₂₅₄) removal may be partly explained by the changes in residual Al. Generally, residual Al increased only a little as the pH increased from 6 to 7, while it increased greatly as the pH increased to 8 (Figure 3E,F).³⁶ At pH 8, the AlO₂⁻ species account for a quite large proportion of all alum species, and thus, it leads to a smaller amount of precipitate (Al(OH)₃) and a lower adsorption capacity for HA. After several breakages, an increase in residual Al was observed for all pH values, which can be ascribed to the alum nanoparticles detached from flocs. These nanosized particles can easily pass the 0.45 μm membrane and be detected by the subsequent ICP-OES. At pH 6, there might be a significant excess of adsorption sites.³⁷ Therefore, the removal rate of HA showed little decrease even after several breakages.

3.4. Floc Structural Analysis. The microscale structures of flocs with and without HA at three different pH values were explored by TEM (Figure S4, Supporting Information). It can be seen that flocs were composed of thousands of nanoscale, nearly spherical particles, the size of which were of several hundred microns (see Figure 1), although the TEM pictures show only very small regions of individual flocs. The size of nanoscale particles was 50–100 nm, and it appeared to be slightly larger at pH 6 (Figure S4A,B, Supporting Information). The presence of HA seemed to have very little effect on the primary particle size, which implied that the alum was first hydrolyzed and formed nanoscale precipitate particles and then interacted with HA, where HA adsorbed on alum precipitates and aggregated to form large flocs. In addition, from the results in Figures 1 and S1 (Supporting Information), it appeared that the flocs with HA (Figure S1A, Supporting Information) were smaller than those without HA (Figure 1B). This may be a

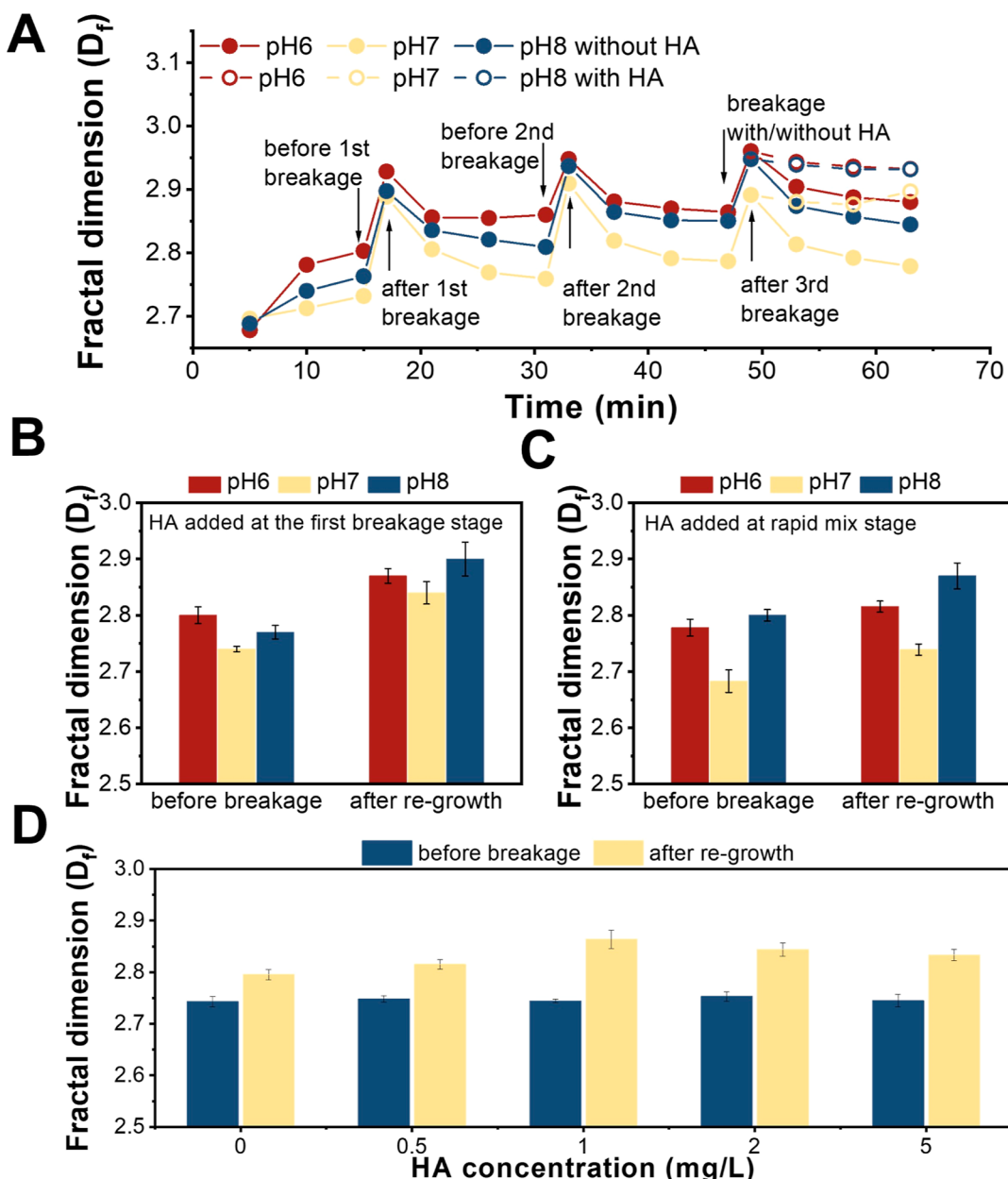


Figure 4. Fractal dimensions (D_f) of flocs through formation, breakage, and regrowth under different pH values with/without HA. (A) Solid circle indicated breakage without HA, and the void circle indicated HA added at the third breakage stage; (B) HA (5 mg/L) was added at the first breakage stage; (C) HA (5 mg/L) was added before coagulant addition; and (D) different doses of HA were added at the third breakage stage under pH 7. Flocs were formed at 50 rpm for 15 min and then broken at 200 rpm for 1 min. Alum dosage was 0.2 mM.

result of the partial surface coverage of the precipitate particles by HA that reduced the connections between particles.

The fractal properties of NOM flocs are useful for understanding the changes in aggregate compaction during floc growth and can help to explain floc structural changes during these periods.¹³ The fractal dimension (D_f) of flocs was continually monitored during the whole coagulation processes (Figure 4A). Generally, for Euclidean objects, the value of D_f will be 1 for a line, 2 for a two-dimensional planar shape, and 3 for a compact three-dimensional shape.³⁸ Flocs are thought to have a D_f between 2 and 3 because of their multilevel structure.³⁹ As the flocs became more compact, the D_f value would increase;¹³ otherwise, it decreased when the flocs form a more elongated chain structure. The cyclical breakage and regrowth of flocs at all pH values showed that the D_f of flocs

gradually increased during the initial growth phase. Once the stirring speed increased to 200 rpm, a dramatical increase in D_f was noticed, indicating that the flocs were broken into more compact pieces.¹³ As the stirring speed turned back to 50 rpm, part of the broken flocs formed new connections with each other, so that the D_f value decreased. It was apparent that the D_f value after the second breakage was higher than that after the first breakage, which suggested that the structure of flocs became more compact with breakage times. When 5 mg/L HA was added at the third breakage, little change of D_f was noticed during the regrowth process. In contrast, the D_f gradually decreased if no HA was added, similar to the previous two cycles. Therefore, it was speculated that HA covered the surface of broken flocs, making it impossible to form new connections with each other for all three pH values.

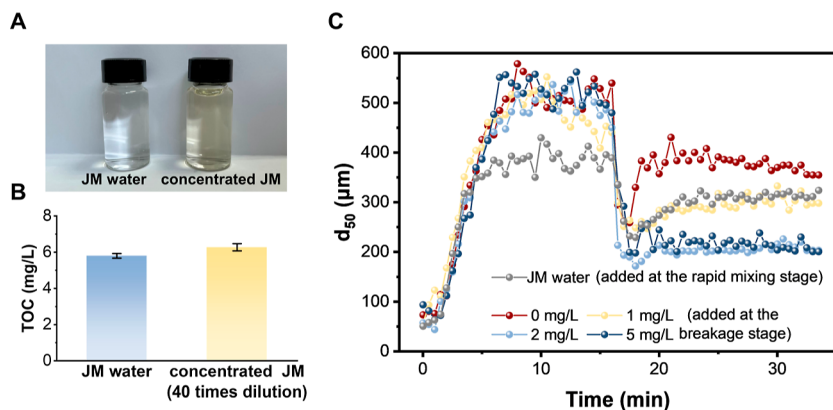


Figure 5. (A) Photographs of JM water and concentrated JM (CJM) water; (B) TOC of JM water and concentrated JM (CJM) water, the CJM water was diluted 40 times; and (C) floc growth, breakage, and regrowth with different doses of CJM added at the breakage stage: 0 mg/L (red), 1 mg/L (yellow), 2 mg/L (light blue), and 5 mg/L (dark blue). The coagulation using JM water was also performed for comparison (gray). Flocs were formed at 50 rpm for 15 min and then broken at 200 rpm for 1 min. Alum dosage was 0.2 mM.

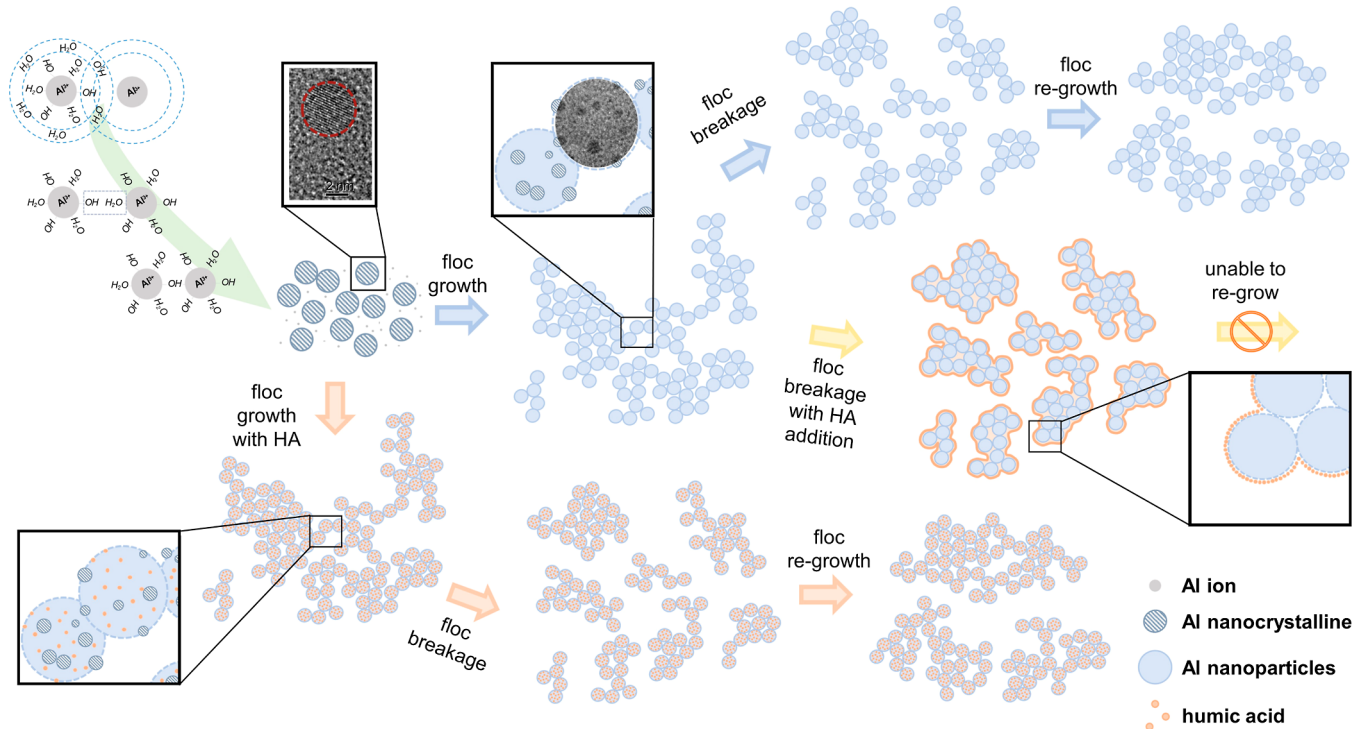


Figure 6. Schematic diagram of floc growth, breakage, and regrowth with or without HA.

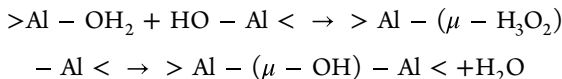
Similar situation also occurred when HA was added at the first breakage. As shown in Figure 4B, the D_f of flocs after breakage was apparently higher than that before breakage. However, when HA was added before coagulant addition, the difference between D_f values (before and after breakage) was not that much (Figure 4C). Besides, the D_f of HA-alum flocs before breakage was lower than that of alum flocs, which was consistent with a previous study.²⁹ The structure of flocs influenced by adding different concentrations of HA during breakage is demonstrated in Figure 4C. D_f of flocs increased from 2.79 to 2.86 as the HA dose increased from 0 to 1 mg/L and decreased slightly to 2.84 as HA concentration increased to 5 mg/L (Figure 4D). This result meant that with the increasing dose of HA, the active points on flocs were gradually covered and led to a lower connection ability between nanoscale particles for floc growth.

3.5. Floc Growth, Breakage, and Regrowth with NOM from Real Surface Water. The abovementioned results indicated that HA added before coagulant addition absorbed on precipitated alum nanoparticles and then aggregated and formed large flocs. When it was added during the floc breakage stage, it covered the activated sites on alum flocs and thus inhibited the floc regrowth. In order to test if this phenomenon is also true for NOM from real surface water, the water sample from JM river was concentrated using nanofiltration membranes (NF90), which can retain nearly 60% of NOM according to our previous studies.⁴⁰ As shown in Figure 5A, the JM water was transparent and colorless, while the concentrated JM (CJM) water was faint yellow. The TOCs of JM water and CJM water were 5.8 ± 0.1 mg/L and 250.8 ± 8.0 mg/L, respectively (Figure 5B). The EEM spectra (Figure S5, Supporting Information) also indicated that the CJM water

had similar fluorescent components to raw JM water. Figure S5C demonstrates the variation of floc size during coagulation when different doses of concentrated JM water were added at the breakage stage. The coagulation using JM water was also performed for comparison. The results are similar to those in Section 3.2. The coagulation using JM water (gray line) led to a lower plateau size compared to DI water (red line). When CJM was added during the breakage stage, the floc size after breakage became smaller with increasing CJM dose. These results evidenced that both HA and NOM exhibited similar behavior during floc growth.

3.6. Floc Growth Mechanism. Over decades, charge neutralization and sweep flocculation are recognized as the predominant coagulation mechanisms. Both describe the process where coagulant species (and contaminants) get close to each other via electrostatic or hydrophobic interaction and aggregate to form large flocs. During coagulation, the zeta potential of the mixture solution (coagulant and contaminants) is regarded as an essential factor affecting the growth of flocs, with a near-zero value leading to the destabilization of the whole system and facilitating the growth of flocs. However, the zeta potential only determined the possibility of flocs approaching each other, and whether the flocs can link and aggregate together, known as the “collision effectiveness”, depends on their active functional groups on the surface. The whole process of floc growth is depicted in Figure 6.

When alum was added to water, it hydrolyzes immediately to form nanoscale primary particles (Figure S4, Supporting Information).^{41,42} $\text{Al}(\text{OH})_6^{3+}$ is converted to $\text{Al}(\text{OH})_n(\text{H}_2\text{O})_{6-n}$ and the inner-sphere hydration water is an active site to react with hydroxyl.^{43,44} Previous studies believed that the water and hydroxyl groups within the inner coordination spheres of the metal ions played an important role in the aggregation of nanoscale primary particles.^{37,45} These types of groups can form $\text{OH}\cdot\text{OH}_2^-$ (written as $\mu\text{-H}_3\text{O}_2$) bridges between Al (III) sites, which further convert to $\mu\text{-OH}$ bridges via a reaction that releases water



With the aggregation of the primary nanoparticles, large flocs are gradually formed during the first several minutes of coagulation. Eventually, the flocs reached an equilibrium of energy-driven structure and size,¹⁵ which depends on the properties of the water (e.g., pH, ionic strength, and alkalinity) and the coagulant dose. With a sudden increase in shear rate, a new, smaller limiting size is rapidly established, and floc breakage occurs at the contact points between nanoscale particles. After breakage, the contact points ($\mu\text{-OH}$ bridges) became inactive, and thus, the flocs cannot regrow to the previous size because of the loss of active binding sites.³⁵ There may also be other interactions between surface sites such as van der Waals attraction or H-bonding, but these interactions should be weaker than the $\mu\text{-OH}$ bonds between particles and, more importantly, be more ready to reform after breakage. Therefore, the number of the $\mu\text{-OH}$ bonds reduces after each breakage cycle, and thus, the regrown flocs would become progressively smaller, as observed in Figures 1 and 2. After three breakage cycles, the regrown flocs have about the same size, irrespective of pH (Figure 1B). This is consistent with the progressive loss of $\mu\text{-OH}$ bonds, so that the bindings become more dependent on physical interactions.

Based on the abovementioned discussion, it is easy to illustrate the inhibition of floc regrowth by the addition of HA. When HA was added before coagulant addition, from the TEM results in Figure S4, Supporting Information, the size of the precipitated nanoparticles did not show much difference with or without HA, indicating that the adsorption of HA occurs mostly after the formation of nanoparticles. However, HA did cause a slight reduction of floc size when comparing the alum flocs (Figure 1A) with alum-HA flocs (Figure S1A, Supporting Information), implying a small inhibitory effect on floc growth because of the partial occupation of active sites on flocs. In contrast, when 5 mg/L HA was added during the floc breakage stage, the floc regrowth was completely prevented (Figure 2A). Considering that the composition of the coagulation systems after floc breakage should be exactly the same no matter when HA was added, it was presumed that the HA coverage on primary precipitate particles and on the surfaces of broken flocs was different (Figure 6). For primary precipitate nanoparticles with a very large surface area, HA with low concentration (5 mg/L) would only partially cover the particle surface, which increased the colloidal stability of the particles and led to a slightly lower final floc size (Figure S1A, Supporting Information) compared to alum flocs (Figure 1B), while for broken flocs, the breakage process has already inactivated some binding sites between alum precipitates, the rest of which was further covered by HA because there was much less available surface than the primary precipitates, thus giving nearly complete colloid stability and preventing floc regrowth (Figure 2A).

The abovementioned two cases represent the (1) conventional coagulation process where the coagulant is added in untreated water containing NOM and (2) high-density sedimentation and sludge recirculation scenarios where old flocs are reused for further NOM adsorption.^{46,47} In the latter case, these old flocs have gone through several to tens of breakage, and the activated functional groups were almost consumed. If the NOM burden is high, the regrowth of these flocs is inhibited. However, if some fresh coagulants are added, they can serve as intermediates to connect the old flocs, so as to maximize the adsorption capacity of the old flocs.²⁴

4. CONCLUSIONS

The binding between precipitate particles consists of both physical and chemical interactions, and the latter is responsible for the irreversible nature of hydroxide floc breakage. During the coagulation of HA, nanoscale precipitate particles are first formed and then significant adsorption of HA takes place, which covers the active sites ($-\text{H}_2\text{O}$) that connect flocs. When HA was added before coagulant addition, the surface coverage on the nanoscale particles was much below saturation, so that the floc growth and the regrowth of broken flocs were not prevented. However, HA added during the floc breakage would be adsorbed mainly on the outer surfaces of the broken flocs, giving more complete coverage and inhibiting floc regrowth. The results of this study highlight the importance of active functional groups on floc growth, reveal the effects of NOM on the growth of fresh flocs and old flocs, and provide an in-depth understanding of the coagulation process. Further study should consider other common coagulants (e.g., Al_{13}) and typical water sources (e.g., algal-laden water).

■ ASSOCIATED CONTENT

SI Supporting Information

The Supporting Information is available free of charge at <https://pubs.acs.org/doi/10.1021/acsestengg.2c00229>.

Floc growth, breakage, and regrowth with HA added before coagulant addition and at the third breakage stage, size distribution of flocs during the breakage stage with different doses of HA, TEM pictures (50,000 \times) of the alum precipitate and alum-humic flocs under different pH values, characterization of JM and concentrated JM water, physical and chemical properties of JM water, and properties of the NF90 membrane ([PDF](#))

■ AUTHOR INFORMATION

Corresponding Author

Wenzheng Yu – State Key Laboratory of Environmental Aquatic Chemistry, Research Center for Eco-Environmental Sciences, Chinese Academy of Sciences, Beijing 100085, China;  orcid.org/0000-0001-9776-8021; Email: wzyu@rcees.ac.cn

Author

Mengjie Liu – State Key Laboratory of Environmental Aquatic Chemistry, Research Center for Eco-Environmental Sciences, Chinese Academy of Sciences, Beijing 100085, China; University of Chinese Academy of Sciences, Beijing 100049, People's Republic of China

Complete contact information is available at:
<https://pubs.acs.org/10.1021/acsestengg.2c00229>

Notes

The authors declare no competing financial interest.

■ ACKNOWLEDGMENTS

This work was also supported by the Key Research and Development Plan of the Ministry of Science and Technology (2019YFC1906501 and 2019YFD1100104).

■ REFERENCES

- (1) Skaf, D. W.; Punzi, V. L.; Rolle, J. T.; Kleinberg, K. A. Removal of micron-sized microplastic particles from simulated drinking water via alum coagulation. *Chem. Eng. J.* **2020**, *386*, 123807.
- (2) Xue, J.; Peldszus, S.; Van Dyke, M. I.; Huck, P. M. Removal of polystyrene microplastic spheres by alum-based coagulation-flocculation-sedimentation (CFS) treatment of surface waters. *Chem. Eng. J.* **2021**, *422*, 130023.
- (3) Sillanpää, M.; Ncibi, M. C.; Matilainen, A.; Vepsäläinen, M. Removal of natural organic matter in drinking water treatment by coagulation: A comprehensive review. *Chemosphere* **2018**, *190*, 54–71.
- (4) Lapointe, M.; Farner, J. M.; Hernandez, L. M.; Tufenkji, N. Understanding and Improving Microplastic Removal during Water Treatment: Impact of Coagulation and Flocculation. *Environ. Sci. Technol.* **2020**, *54*, 8719–8727.
- (5) Wu, B.; Li, J.; Gan, Y.; Li, H.; Dong, L.; Zhang, S. Titanium Coagulation Simplified Removal Procedure and Alleviated Membrane Fouling in Treatment of Antimony-Containing Wastewater. *ACS ES&T Engg* **2021**, *1*, 1094–1103.
- (6) Tomasi, I. T.; Machado, C. A.; Boaventura, R. A. R.; Botelho, C. M. S.; Santos, S. C. R. Tannin-based coagulants: Current development and prospects on synthesis and uses. *Sci. Total Environ.* **2022**, *822*, 153454.
- (7) Gan, Y.; Li, J.; Zhang, L.; Wu, B.; Huang, W.; Li, H.; Zhang, S. Potential of titanium coagulants for water and wastewater treatment: Current status and future perspectives. *Chem. Eng. J.* **2021**, *406*, 126837.
- (8) Ahmad, A.; Kurniawan, S. B.; Ahmad, J.; Alias, J.; Marsidi, N.; Said, N. S. M.; Yusof, A. S. M.; Buhari, J.; Ramli, N. N.; Rahim, N. F. M.; Abdullah, S. R. S.; Othman, A. R.; Hasan, H. A. Dosage-based application versus ratio-based approach for metal- and plant-based coagulants in wastewater treatment: Merits, limitations, and applicability. *J. Clean. Prod.* **2022**, *334*, 130245.
- (9) Gan, Y.; Wang, X.; Zhang, L.; Wu, B.; Zhang, G.; Zhang, S. Coagulation removal of fluoride by zirconium tetrachloride: Performance evaluation and mechanism analysis. *Chemosphere* **2019**, *218*, 860–868.
- (10) Reckhow, D. A.; Singer, P. C. The Removal of Organic Halide Precursors by Preozonation and Alum Coagulation. *J. Am. Water Works Assoc.* **2019**, *111*, 62–67.
- (11) Duan, J.; Gregory, J. Coagulation by hydrolysing metal salts. *Adv. Colloid Interface Sci.* **2003**, *100-102*, 475–502.
- (12) Yukselen, M. A.; Gregory, J. The reversibility of floc breakage. *Int. J. Miner. Process.* **2004**, *73*, 251–259.
- (13) Jarvis, P.; Jefferson, B.; Parsons, S. A. Breakage, Regrowth, and Fractal Nature of Natural Organic Matter Flocs. *Environ. Sci. Technol.* **2005**, *39*, 2307–2314.
- (14) McCurdy, K.; Carlson, K.; Gregory, D. Floc morphology and cyclic shearing recovery: comparison of alum and polyaluminum chloride coagulants. *Water Res.* **2004**, *38*, 486–494.
- (15) Solomentseva, I.; Bárány, S.; Gregory, J. The effect of mixing on stability and break-up of aggregates formed from aluminum sulfate hydrolysis products. *Colloids Surf., A* **2007**, *298*, 34–41.
- (16) Gonzalez-Torres, A.; Putnam, J.; Jefferson, B.; Stuetz, R. M.; Henderson, R. K. Examination of the physical properties of *Microcystis aeruginosa* flocs produced on coagulation with metal salts. *Water Res.* **2014**, *60*, 197–209.
- (17) Sun, H.; Jiao, R.; Xu, H.; An, G.; Wang, D. The influence of particle size and concentration combined with pH on coagulation mechanisms. *J. Environ. Sci.* **2019**, *82*, 39–46.
- (18) Yu, W.; Gregory, J.; Campos, L. C.; Graham, N. Dependence of floc properties on coagulant type, dosing mode and nature of particles. *Water Res.* **2015**, *68*, 119–126.
- (19) Wang, Y.; Gao, B.-Y.; Xu, X.-M.; Xu, W.-Y.; Xu, G.-Y. Characterization of floc size, strength and structure in various aluminum coagulants treatment. *J. Colloid Interface Sci.* **2009**, *332*, 354–359.
- (20) Jarvis, P.; Jefferson, B.; Parsons, S. A. Floc structural characteristics using conventional coagulation for a high doc, low alkalinity surface water source. *Water Res.* **2006**, *40*, 2727–2737.
- (21) Li, Y.; Xu, L.; Shi, T.; Yu, W. The influence of various additives on coagulation process at different dosing point: From a perspective of structure properties. *J. Environ. Sci.* **2021**, *101*, 168–176.
- (22) de Vicente, I.; Huang, P.; Andersen, F. Ø.; Jensen, H. S. Phosphate Adsorption by Fresh and Aged Aluminum Hydroxide. Consequences for Lake Restoration. *Environ. Sci. Technol.* **2008**, *42*, 6650–6655.
- (23) Yu, W.; Gregory, J.; Campos, L. The effect of additional coagulant on the re-growth of alum-kaolin flocs. *Sep. Purif. Technol.* **2010**, *74*, 305–309.
- (24) Yu, W.-Z.; Gregory, J.; Campos, L. Breakage and Regrowth of Al-Humic Flocs - Effect of Additional Coagulant Dosage. *Environ. Sci. Technol.* **2010**, *44*, 6371–6376.
- (25) Van Benschoten, J. E.; Edzwald, J. K. Chemical aspects of coagulation using aluminum salts-I. Hydrolytic reactions of alum and polyaluminum chloride. *Water Res.* **1990**, *24*, 1519–1526.
- (26) Wang, Z.; Li, Y.; Hu, M.; Lei, T.; Tian, Z.; Yang, W.; Yang, Z.; Graham, N. J. D. Influence of DOM characteristics on the flocculation removal of trace pharmaceuticals in surface water by the successive dosing of alum and moderately hydrophobic chitosan. *Water Res.* **2022**, *213*, 118163.

- (27) Davis, C. C.; Edwards, M. Role of Calcium in the Coagulation of NOM with Ferric Chloride. *Environ. Sci. Technol.* **2017**, *51*, 11652–11659.
- (28) Geng, C.-X.; Cao, N.; Xu, W.; He, C.; Yuan, Z.-W.; Liu, J.-W.; Shi, Q.; Xu, C.-M.; Liu, S.-T.; Zhao, H.-Z. Molecular Characterization of Organics Removed by a Covalently Bound Inorganic-Organic Hybrid Coagulant for Advanced Treatment of Municipal Sewage. *Environ. Sci. Technol.* **2018**, *52*, 12642–12648.
- (29) Zhong, R.; Zhang, X.; Xiao, F.; Li, X.; Cai, Z. Effects of humic acid on physical and hydrodynamic properties of kaolin flocs by particle image velocimetry. *Water Res.* **2011**, *45*, 3981–3990.
- (30) Zhang, X.; Graham, N.; Xu, L.; Yu, W.; Gregory, J. The Influence of Small Organic Molecules on Coagulation from the Perspective of Hydrolysis Competition and Crystallization. *Environ. Sci. Technol.* **2021**, *55*, 7456–7465.
- (31) Su, Z.; Yu, W.; Liu, T.; Li, X.; Graham, N. J. D.; Lu, Y.; Wiesner, M. R. Discovery of Welcome Biopolymers in Surface Water: Improvements in Drinking Water Production. *Environ. Sci. Technol.* **2021**, *55*, 2076–2086.
- (32) Su, Z.; Liu, T.; Li, X.; Graham, N.; Yu, W. Beneficial impacts of natural biopolymers during surface water purification by membrane nanofiltration. *Water Res.* **2021**, *201*, 117330.
- (33) Yu, W.; Hu, C.; Liu, H.; Qu, J. Effect of dosage strategy on Al-humic flocs growth and re-growth. *Colloids Surf, A* **2012**, *404*, 106–111.
- (34) Ehrl, L.; Soos, M.; Morbidelli, M. Dependence of Aggregate Strength, Structure, and Light Scattering Properties on Primary Particle Size under Turbulent Conditions in Stirred Tank. *Langmuir* **2008**, *24*, 3070–3081.
- (35) Yu, W.; Gregory, J.; Campos, L. C. Breakage and re-growth of flocs: Effect of additional doses of coagulant species. *Water Res.* **2011**, *45*, 6718–6724.
- (36) Pernitsky, D.; Edzwald, J. Solubility of polyaluminium coagulants. *J. Water Supply: Res. Technol.—AQUA* **2003**, *52*, 395–406.
- (37) Wu, M.; Yu, W.; Qu, J.; Gregory, J. The variation of flocs activity during floc breakage and aging, adsorbing phosphate, humic acid and clay particles. *Water Res.* **2019**, *155*, 131–141.
- (38) Waite, T. D. Measurement and implications of floc structure in water and wastewater treatment. *Colloids Surf, A* **1999**, *151*, 27–41.
- (39) Wu, R. M.; Lee, D. J.; Waite, T. D.; Guan, J. Multilevel Structure of Sludge Flocs. *J. Colloid Interface Sci.* **2002**, *252*, 383–392.
- (40) Siddique, M. S.; Xiong, X.; Yang, H.; Maqbool, T.; Graham, N.; Yu, W. Dynamic variations in DOM and DBPs formation potential during surface water treatment by ozonation-nanofiltration: Using spectroscopic indices approach. *Chem. Eng. J.* **2022**, *427*, 132010.
- (41) Amirtharajah, A.; Mills, K. M. Rapid-mix design for mechanisms of alum coagulation. *J. AWWA* **1982**, *74*, 210–216.
- (42) Yu, W.; Xu, L.; Lei, K.; Gregory, J. Effect of crystallization of settled aluminum hydroxide precipitate on “dissolved Al”. *Water Res.* **2018**, *143*, 346–354.
- (43) Nordin, J. P.; Sullivan, D. J.; Phillips, B. L.; Casey, W. H. An ¹⁷O-NMR Study of the Exchange of Water on $\text{AlOH}(\text{H}_2\text{O})_{52+}(\text{aq})$. *Inorg. Chem.* **1998**, *37*, 4760–4763.
- (44) Phillips, B. L.; Tossell, J. A.; Casey, W. H. Experimental and Theoretical Treatment of Elementary Ligand Exchange Reactions in Aluminum Complexes. *Environ. Sci. Technol.* **1998**, *32*, 2865–2870.
- (45) Li, X.; Graham, N. J. D.; Deng, W.; Liu, M.; Liu, T.; Yu, W. The formation of planar crystalline flocs of $\gamma\text{-FeOOH}$ in Fe(II) coagulation and the influence of humic acid. *Water Res.* **2020**, *185*, 116250.
- (46) Dayaratne, H. N. P.; Angove, M. J.; Jeong, S.; Aryal, R.; Paudel, S. R.; Mainali, B. Effect of temperature on turbidity removal by coagulation: Sludge recirculation for rapid settling. *J. Water Proc. Eng.* **2022**, *46*, 102559.
- (47) Chen, Z.; Yang, B.; Wen, Q.; Chen, C. Evaluation of enhanced coagulation combined with densadeg-ultrafiltration process in treating secondary effluent: Organic micro-pollutants removal, genotoxicity reduction, and membrane fouling alleviation. *J. Hazard. Mater.* **2020**, *396*, 122697.